CELL REGULATION, Vol. 1, 921–936, November 1990

Microtubule perturbation inhibits intracellular transport of an apical membrane glycoprotein in a substrate-dependent manner in polarized Madin-Darby canine kidney epithelial cells

Marja J.A.H. van Zeijl and Karl S. Matlin
Department of Anatomy and Cellular Biology
Harvard Medical School
Boston, Massachusetts 02115

The effects of microtubule perturbation on the transport of two different viral glycoproteins were examined in infected Madin-Darby canine kidney (MDCK) cells grown on both permeable and solid substrata. Quantitative biochemical analysis showed that the microtubule-depolymerizing drug nocodazole inhibited arrival of influenza hemagglutinin on the apical plasma membrane in MDCK cells grown on both substrata. In contrast, the microtubule-stabilizing drug taxol inhibited apical appearance of hemagglutinin only when MDCK cells were grown on permeable substrata. On the basis of hemagglutinin mobility on sodium dodecyl sulfate gels and its sensitivity to endo H, it was evident that nocodazole and taxol arrested hemagglutinin at different intracellular sites. Neither drug caused a significant increase in the amount of hemagglutinin detected on the basolateral plasma membrane domain. In addition, neither drug had any noticeable effect on the transport of the vesicular stomatitis virus (VSV)-G protein to the basolateral surface. These results shed light on previous conflicting reports using this model system and support the hypothesis that microtubules play a role in the delivery of membrane glycoproteins to the apical, but not the basolateral, domain of epithelial cells.

Introduction

Epithelia form a barrier between the internal milieu and the outside of the organs that they line. Epithelial cells are polarized to perform this barrier function properly. The plasma membrane of epithelial cells is divided into an apical domain, or free surface, and a basolateral domain, in contact with the substratum. Each domain has a unique composition of proteins and lipids. To generate and maintain this polarity, epithelial cells must sort the membrane components directed to each domain (Matlin, 1986a; Caplan and Matlin, 1989; Rodriguez-Boulan and Nelson, 1989). The mechanisms by which sorting occurs are poorly understood.

The process of sorting can be conveniently studied in Madin-Darby canine kidney cells (MDCK), an epithelial cell line that forms polarized monolayers in culture (Simons and Fuller, 1985). When MDCK cells are infected with enveloped viruses, budding of these viruses occurs in a polarized fashion. Influenza virus, for example, buds predominantly from the apical domain, whereas vesicular stomatitis virions (VSV) have been shown to bud primarily from the basolateral side (Rodriguez-Boulan and Sabatini, 1978). This polarized budding is a consequence of the polarized insertion of the viral spike glycoproteins hemagglutinin and the VSV-G protein, respectively (Rodriguez-Boulan and Pendergast, 1980). The viral glycoproteins are transported with similar kinetics and traverse the same biosynthetic pathways as endogenous proteins (Lisanti *et al.,* 1989). Hence, the sorting mechanisms for the viral glycoproteins can be assumed to be no different from those for endogenous proteins.

In MDCK cells the segregation of apically and basolaterally targeted proteins has been shown to take place at the final stage of transit, possibly in a specialized part of the Golgi complex known as the trans-Golgi network (TGN; Matlin and Simons, 1984; Simons and Fuller, 1985; Griffiths and Simons, 1986). After separation of the proteins, the vesicles containing the sorted proteins are delivered to the correct plasma membrane domains. Although it is conceivable that vesicles targeted to the plasma membrane domains simply diffuse to their destinations, it is also possible that the cytoskeleton plays a role. Of the cytoskeletal components, microtubules are of particular interest because of their established functions in other cellular processes. Microtubules mediate the polarized transport of vesicles in neuronal cells (Schnapp *et al.,* 1985). Furthermore, in most cells, micro-

tubules are closely associated with the Golgi complex, the site of sorting. Upon drug-induced depolymerization of microtubules, the Golgi complex fragments into individual stacks of cisternae and disperses (Rogalski and Singer, 1984; Ho *et al.,* 1989; Turner and Tartakoff, 1989), suggesting that microtubules play a role in the maintenance of the three-dimensional structure of the Golgi complex (Stults *et al.,* 1989; Kreis, 1990).

With the use of various microtubule-perturbing drugs, the role of microtubules in protein transport has been extensively studied in different cell systems (Busson-Mabillot *et al.,* 1982; Rogalski *et al.,* 1984; Achler *et al.,* 1989; Stults *et al.,* 1989). Nocodazole, a depolymerizing drug (De Brabander *et al.,* 1976), and taxol, a hyperpolymerizing drug (De Brabander *et al.,* 1981; Horwitz *et al.,* 1986), have been used to examine the role of the microtubular cytoskeleton in sorting in MDCK cells. Salas *et al.* (1986) originally reported that microtubule-perturbing drugs had no effect on the sorting of either apical or basolateral viral glycoproteins. In contrast, Rindler *et al.* (1987) found that the apical protein hemagglutinin was delivered randomly to both the apical and the basolateral domains after disruption of the microtubular cytoskeleton, whereas sorting of VSV-G protein to the basolateral domain was unaffected. Reasons for the dramatic differences between these studies were not obvious.

To clarify this issue, we report here a biochemical analysis of influenza hemagglutinin and VSV-G protein transport and sorting in MDCK cells after perturbation of the microtubular cytoskeleton by drug treatment. We find that both transport and processing of hemagglutinin, but not of VSV-G protein, are affected by nocodazole and taxol. However, missorting of hemagglutinin to the basolateral domain does not take place. These effects are dependent on the type of growth substratum, emphasizing the importance of physiological growth conditions for in vitro studies of epithelial polarity.

Results

Spatial distribution of the microtubular cytoskeleton in MDCK cells grown on solid or permeable substrata

MDCK cells may be grown on both solid (impermeable) or permeable substrata, depending on experimental requirements. To obtain an impression of the spatial distribution of the microtubular cytoskeleton under different culture conditions, we visualized microtubules by fluorescence microscopy in cells grown on either glass coverslips or permeable nitrocellulose acetate (Millicell HA) supports.

MDCK cells grown on glass coverslips were stained for tubulin and scanned with a confocal laser microscope (Bacallao and Stelzer, 1989; Figure 1). The cells were ~13 μm tall. At the top of the cells, microtubules were observed in an apical cap (Figure 1, a and b). The nucleus was seen as a dark sphere lying below the apical cap and surrounded by a network of microtubules (Figure 1, c and d). These lateral microtubules had a higher density on one side of the nucleus, where they formed a criss-cross pattern (Figure 1c). Some microtubules were observed in the basal side of the cell, but their concentration was less than in the apical side of the cell (Figure 1e).

In contrast, MDCK cells grown to confluence on permeable supports were ~17 μm tall (Figure 2). This increase in height appeared to be compensated for by a decrease in the width of the cells. Consequently, more cytoplasm was present above the nucleus in cells grown on permeable supports than beside the nucleus as in MDCK cells grown on glass coverslips. The apical cap seen in glass-grown cells was also evident in cells grown on permeable supports (Figure 2a). This cap was usually the brightest part of the cell. In the plane of the nucleus, which was seen as a dark circle, a punctate stain was found (Figure 2b), suggesting a vertical orientation of the microtubules at this level (Bacallao *et al.,* 1989). Below the nucleus, in the most basal part of the cells, microtubules formed a loose basal network (Figure 2c).

Thus, it appeared that the microtubular cytoskeleton in MDCK cells grown on permeable substrata was more polarized along the apical-basal axis than that in MDCK cells grown on glass coverslips.

Effects of nocodazole and taxol on the microtubular cytoskeleton in MDCK cells

To determine the optimal concentration of the microtubule-perturbing drugs, we used immunofluorescence to examine the effects of nocodazole and taxol on microtubules in MDCK cells grown on glass coverslips. In preliminary studies, we observed that at 37°C taxol initiated microtubule hyperpolymerization after 3 h, and nocodazole started to depolymerize microtubules after 30 min (data not shown). We therefore employed standard incubation times of 4 h for taxol and 1 h for nocodazole in subsequent experiments.

The effect of taxol on microtubules, as noted by the hyperpolymerization of microtubules in

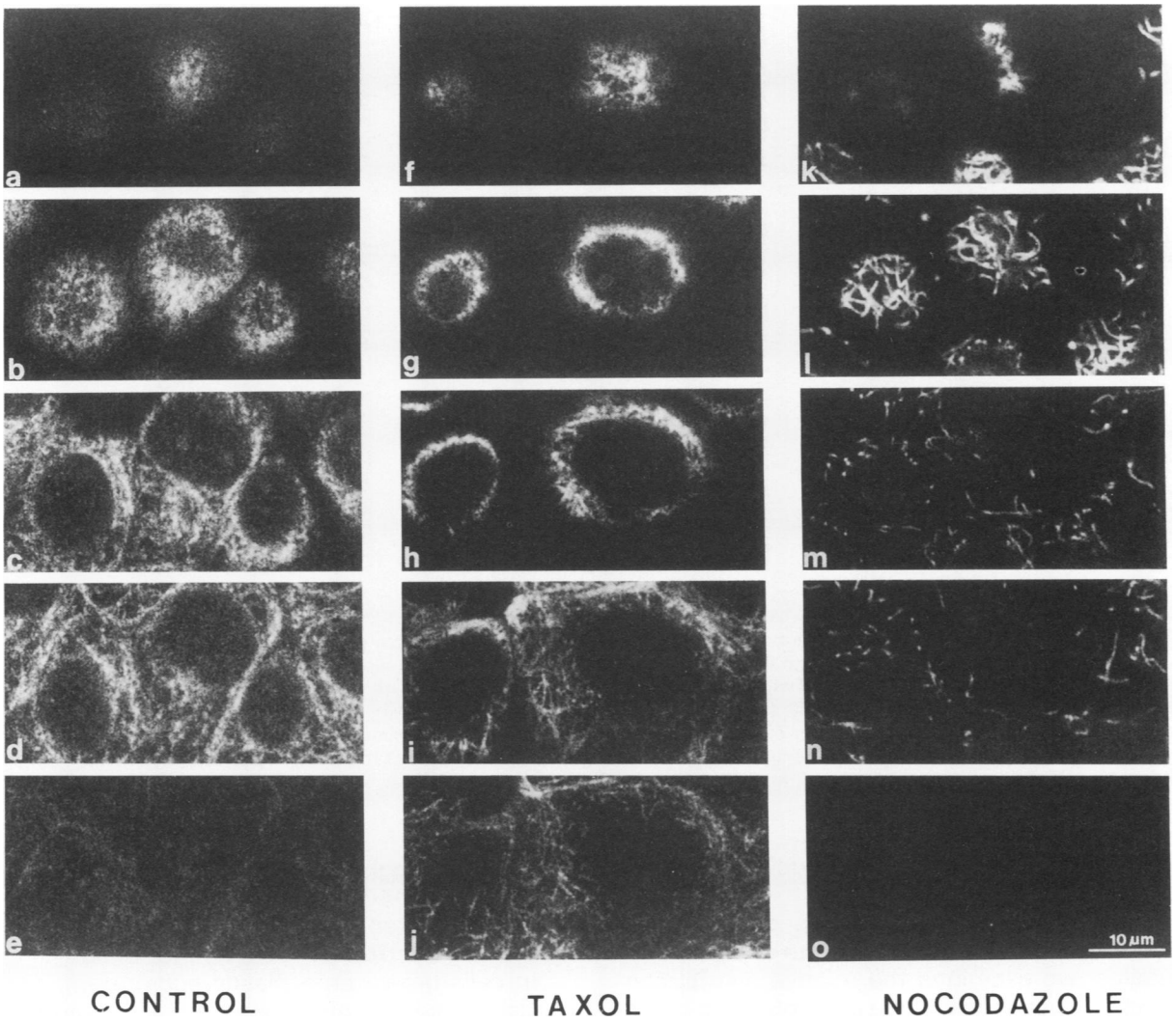

Figure 1. **Spatial distribution of microtubules in MDCK cells grown on glass coverslips and treated with taxol or nocodazole.** MDCK cells were grown on glass coverslips, treated with (a–e) 0.1% DMSO for 4 h, (f–j) 10 μM taxol for 4 h, or (k–o) 10 μg/ml nocodazole for 1 h, permeabilized; and fixed with paraformaldehyde as described in Methods. Microtubules were visualized using B-5-1-2, a monoclonal antibody against α-tubulin, followed by an FITC-conjugated secondary antibody. Optical sections were taken at 2-μm intervals along the vertical axis of the cells with a confocal laser microscope. Sections are shown from the apical (a, f, k) to the basal side (e, j, o) of the cells. The distribution of microtubules between control and taxol-treated cells differs very little, whereas most of the nocodazole-resistant microtubules are found in the apical part of the cell. Bar = 10 μm.

the periphery of the cell, was optimal at 10 μM. Nocodazole at 10 μg/ml resulted in optimal depolymerization at 37°C (data not shown). Based on these results, incubations of 10 μg/ml nocodazole for 1 h and 10 μM taxol for 4 h at 37°C were chosen as standard.

To assess the effects of the drugs on the spatial organization of the microtubular cytoskeleton, we administered taxol and nocodazole to MDCK cells grown on both glass and nitrocellulose acetate supports and examined the cells by confocal microscopy (Figures 1, f–o, and 2, d–i). In taxol-treated cells, more microtubules were visible throughout the cells compared with the control. In taxol-treated cells grown on both substrata, no changes were observed in overall subcellular distribution of the microtubules compared with the control (Figures 1, f–j, and 2, d–f). In nocodazole-treated cells, a large reduction of microtubules was seen in cells grown on both substrata. Most of the nocodazole-resistant microtubules were present in the apical part of the cells (Figures 1, k–l, and 2g). These apically localized nocodazole-resistant microtubules could represent the short residues of the lateral microtubules that remained after de-

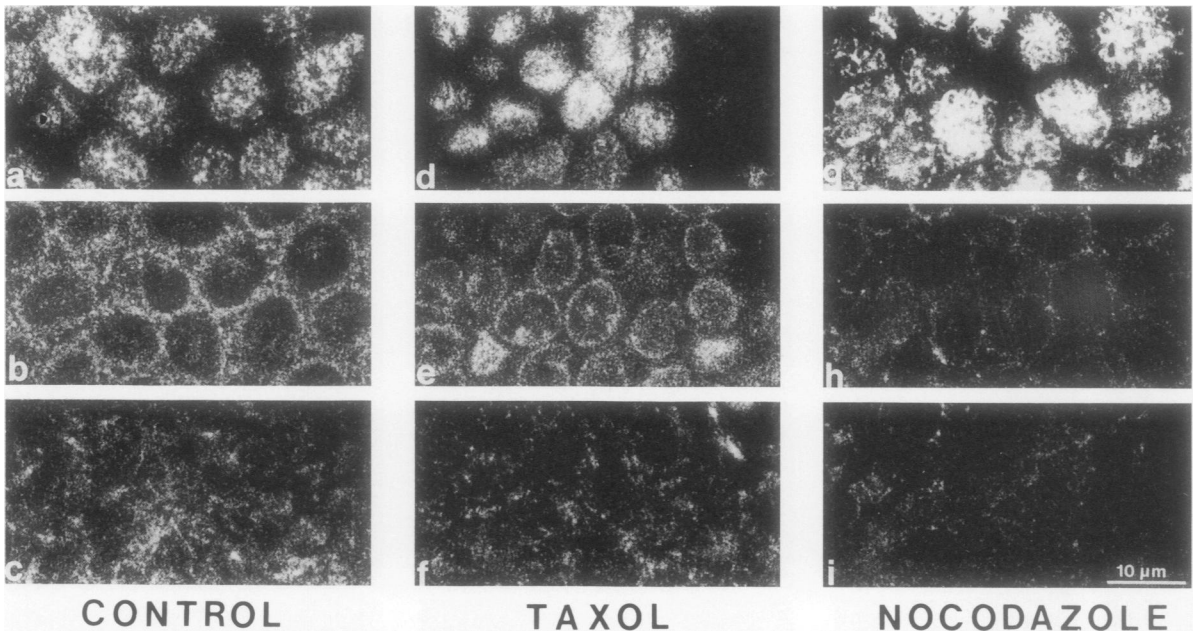

Figure 2. **Spatial distribution of microtubules in MDCK cells grown on permeable supports.** MDCK cells were grown on Millicell HA culture supports, treated with (a–c) 0.1% DMSO for 4 h, (d–f) 10 μM taxol for 4 h, or (g–i) 10 μg/ml nocodazole for 1 h at 37°C; permeabilized; and fixed with paraformaldehyde as described in Methods. Microtubules were visualized with the α-tubulin specific monoclonal B-5-1-2, followed by an FITC-conjugated secondary antibody. Optical sections were taken at 6-μm intervals along the vertical axis of the cells with a confocal laser microscope. Three representative sections are shown: the top of the cells, showing the apical cap (a, d, and g); the middle part of the cells, at the level of the nucleus (b, e, and h); and the most basal section of the cell (c, f, and i). See text for details. Bar = 10 μm.

polymerization from the plus-ends (R. Bacallao, personal communication).

To quantitatively evaluate the action of the drugs on the polymerization state of the microtubules, we examined the relative distribution of tubulin between soluble and polymeric pools of extracts from control and drug-treated cells by Western blotting. As shown in Figure 3, after treatment of cells with 10 μg/ml nocodazole, >90% of tubulin was soluble (Figure 3, lanes 3 and 4) compared with ~50% in control cells (Figure 3, lanes 1 and 2). Tubulin in taxol-treated cells was found almost exclusively in the polymeric form (Figure 3, lanes 5 and 6). There was a slight difference in the tubulin distribution between drug-treated cells grown on plastic and cells grown on permeable supports (compare panel a to panel b of Figure 3, lanes 4 and 5).

Effect of nocodazole and taxol on surface expression of the viral glycoprotein hemagglutinin

Before examining the effects of the microtubule-perturbing drugs on sorting, we determined whether the overall level of expression of newly synthesized hemagglutinin on the cell surface was changed by the drug treatments. Arrival of labeled hemagglutinin on the surface of infected cells was monitored by trypsin proteolysis and was quantitated after sodium dodecyl sulfate (SDS) gel electrophoresis (see Methods).

In cells grown on a plastic substratum, nocodazole significantly inhibited cell-surface appearance of hemagglutinin (Figure 4a). After 60 min of chase, only ~40% of labeled hemagglutinin had reached the plasma membrane, compared with >60% in controls. Inhibition of hemagglutinin transport was kinetic in nature: after prolonged chase times in the presence of nocodazole, more hemagglutinin reached the cell surface. It takes several hours for the surface expression to completely plateau, and, because some of the intracellular hemagglutinin is degraded, control levels are never reached (data not shown). In this experiment, with MDCK cells grown on a plastic substratum, trypsin was only applied to the apical side of the cells because the presence of tight junctions prevented trypsin from reaching the basolateral side. Because trypsin treatment after opening of the tight junctions failed to increase the fraction of cleaved hemagglutinin (data not shown), we concluded that the uncleaved hemagglutinin was located intracellularly and not on the basolateral plasma membrane.

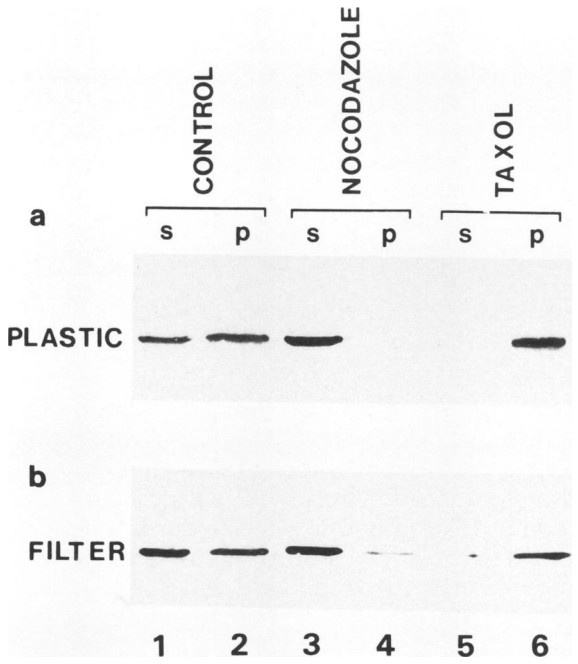

Figure 3. **Distribution of tubulin in polymeric and soluble pools in drug-treated cells.** MDCK cells grown on either plastic petri dishes (plastic; a) or Millicell HA supports (filter; b), were treated with 0.1% DMSO for 4 h (lanes 1 and 2), 10 μg/ml nocodazole for 1 h (lanes 3 and 4), or 10 μM taxol for 4 h (lanes 5 and 6) at 37°C. Soluble (s) tubulin was extracted with 0.1% Triton X-100; insoluble residues containing polymeric tubulin (p) were solubilized in 0.5% SDS (see Methods). Equal amounts of protein from each fraction were loaded on a 10% SDS polyacrylamide gel. After separation, the proteins were transferred to Immobilon PVDF membrane, and probed with B-5-1-2, directed against α-tubulin. The location of the antibody was visualized with an HRP-conjugated secondary antibody, followed by reaction with diaminobenzidine in the presence of H_2O_2.

In contrast with nocodazole, taxol treatment had no effect on the rate or extent of hemagglutinin transport to the surface of cells grown on plastic substrata (Figure 4a).

In cells grown on permeable substrata, surface expression of hemagglutinin was also inhibited by nocodazole (Figure 4b). The level of inhibition was similar to that seen in nocodazole-treated cells grown on plastic. With longer incubation times, almost all of the labeled hemagglutinin reached the cell surface (the degradation of hemagglutinin was not observed), showing that nocodazole caused a kinetic inhibition also in cells grown on a permeable substratum. Surprisingly, taxol treatment of cells grown on permeable substrata did block the arrival of hemagglutinin on the cell surface, in contrast to the results with taxol-treated MDCK cells grown on plastic. The kinetics and extent of inhibition by taxol were similar to those seen with nocodazole treatment (Figure 4b).

Thus, both nocodazole and taxol perturbed intracellular transport of hemagglutinin. However, the effect of taxol on transport seemed to depend on the growth substratum.

Microtubule-perturbing drugs disrupt apical transport of hemagglutinin

To analyze the effects of the microtubule-perturbing drugs on the polarity of hemagglutinin expression, we infected cells grown on permeable supports with influenza virus and treated with drugs or DMSO. The polarity of hemagglutinin expression was assayed by differential trypsinization of either the apical or the basolateral domain. After immunoprecipitation, the oligosaccharide processing and the polarity of transport of hemagglutinin was monitored by SDS-gel electrophoresis (Figures 5 and 6).

Hemagglutinin, synthesized in the endoplasmic reticulum as a protein of 68 000 Da (HAo), was seen after a 5-min pulse-label (Figures 5a and 6a, lanes 1 and 2). After a chase of 30 min, the mature form of hemagglutinin (HA), running slightly slower than HAo, and the trypsin cleavage products, HA1 and HA2, were seen, indicating that hemagglutinin had passed through the Golgi complex and had arrived at the cell surface (Figures 5a and 6a, lanes 3 and 4). At 60 min of chase, most hemagglutinin cleavage occurred when trypsin was added at the apical side of the cells (Figures 5a and 6a, lanes 5). Some cleaved hemagglutinin was also detectable when trypsin was added to the basolateral compartment (Figures 5a and 6a, lanes 4 and 6). Most of this probably represented a background of endogenous cleavage rather than actual expression of significant quantities of hemagglutinin on the basolateral side (see "Quantitation and Statistical Analysis" in Methods).

After nocodazole treatment, the amount of hemagglutinin cleaved by apically added trypsin was reduced (Figure 5a, lane 11), whereas the amount of cleavage observed on the basolateral side was unchanged compared with the control (Figure 5, a [lane 12] and b). Taxol treatment also reduced apical membrane expression of hemagglutinin but had no effect on basolateral expression (Figure 6a, lanes 11 and 12).

These results suggested that drug treatment selectively inhibited hemagglutinin transport to the apical domain. Statistical analysis of several experiments confirmed this conclusion: the ratio of cleaved hemagglutinin detected on the apical domain over that detected on the basolateral

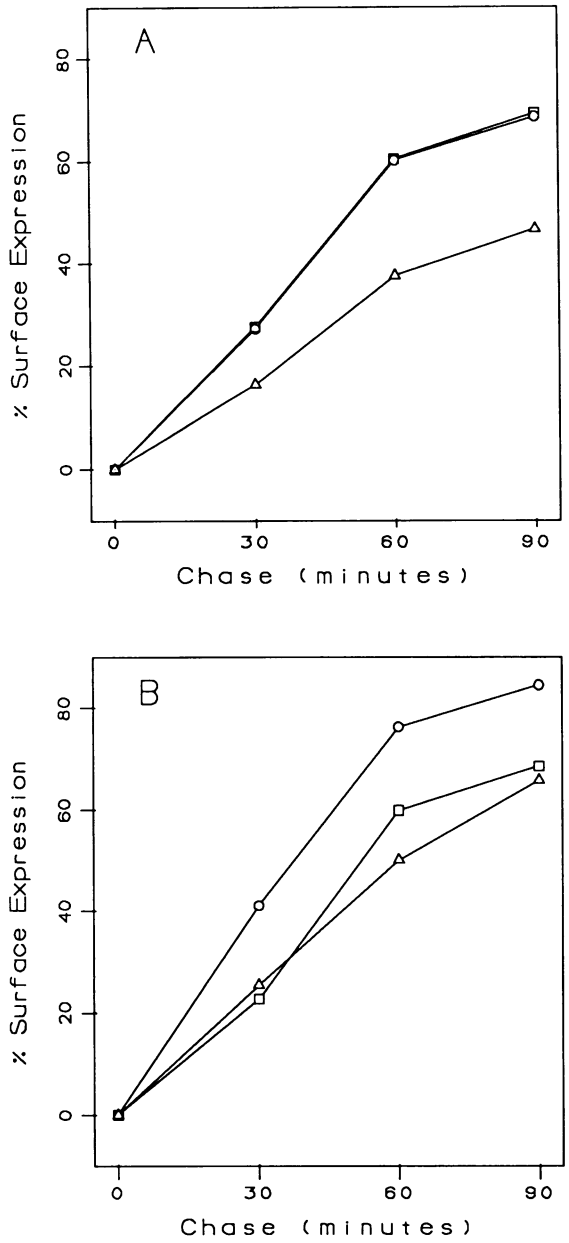

Figure 4. **Total surface expression of hemagglutinin in MDCK cells grown on solid and permeable substrata.** MDCK cells infected with influenza virus were grown on plastic petri dishes (A) or Millicell HA culture supports (B) and treated with 0.1% DMSO for 4 h (○), 10 μM taxol for 4 h (□), or 10 μg/ml nocodazole for 1 h (△). After a 5-min pulse with 50 μCi [^{35}S]-methionine, the cells were incubated with excess unlabeled methionine for the times indicated. Cells were put on ice and trypsinized to cleave hemagglutinin on the cell surface. Trypsin was added to both sides of the cells grown on the Millicell HA culture supports. The basal surface of the cells grown on plastic petri dishes was inaccessible to trypsin. Cultures grown on plastic with the tight junctions opened did not show increased trypsin cleavage (see also text). After lysis, hemagglutinin was immunoprecipitated and the immunoprecipitates were analyzed by SDS gel electrophoresis. The percent of hemagglutinin expressed on the cell surface was quantitated as described in Methods. A representative experiment is shown.

domain was decreased in drug-treated cells compared with the controls (Figures 5b and 6b). This reduction in polarity of expression could be attributed solely to a decrease in delivery to the apical domain. Random delivery of hemagglutinin to both plasma membrane domains, which would have led to an increase in the amount of the hemagglutinin at the basolateral membrane, was not observed.

Processing of intracellularly arrested hemagglutinin

The reduction in apical hemagglutinin expression in drug-treated cells was balanced by accumulation inside the cell. This was evident from the increased amount of uncleaved hemagglutinin in nocodazole-treated cells (Figure 5a, lanes 9–12) compared with the control (Figure 5a, lanes 3–6). Uncleaved hemagglutinin was detected in two bands of different molecular weight. The amount of hemagglutinin in the lower band of the two, running slightly faster than HAo, was notably increased in nocodazole-treated cells (Figure 5a, lanes 9–12). The hemagglutinin in this band was endoglycosidase H (endoH) sensitive (data not shown), indicating it had not acquired complex sugars and suggesting it had not reached the medial compartment of the Golgi complex. The slightly increased mobility of this band relative to that seen after pulse-labeling could be due to extensive mannose trimming of the oligosaccharide side chains (Balch *et al.,* 1986). Hemagglutinin was also present in the terminally glycosylated, more slowly migrating band, as in the control, suggesting that the hemagglutinin in this band was either in the Golgi complex or on its way to the plasma membrane. In contrast, the intracellularly arrested hemagglutinin in taxol-treated cells appeared to be terminally glycosylated (Figure 6a, lanes 9–12). This suggested that hemagglutinin in taxol-treated cells accumulated at a late stage in the transport pathway, presumably in or beyond the trans-Golgi. Thus, the hemagglutinin that accumulated intracellularly appeared to be differently glycosylated in taxol-treated cells than in nocodazole-treated MDCK cells.

Microtubule-perturbing drugs do not disrupt basolateral transport of VSV-G

To examine whether transport of proteins to the basolateral domain was affected by nocodazole or taxol, we performed similar experiments with VSV-infected cells. Because VSV infection required basolateral addition of the virus (Fuller *et al.,* 1984), the cells were grown on culture

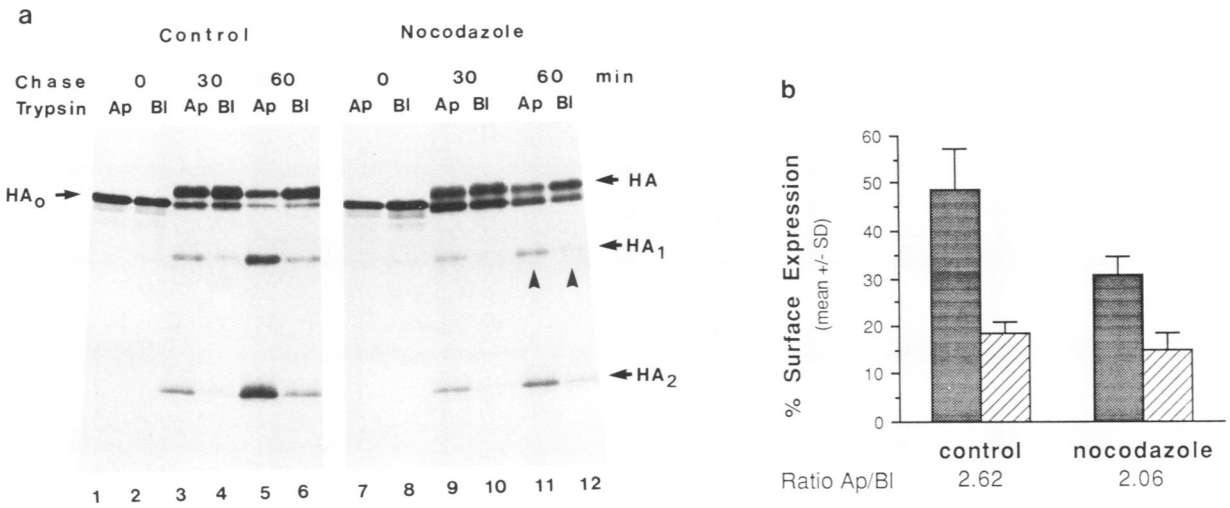

Figure 5. **Transport of hemagglutinin to the apical domain is inhibited by nocodazole.** (a) MDCK cells grown on Millicell HA culture supports were infected with influenza virus and treated with 0.1% DMSO (control) or 10 μg/ml nocodazole for 1 h at 37°C before pulse-labeling. After a 5-min pulse with 50 μCi [^{35}S]-methionine, cells were chased for 0 (lanes 1 and 2, 7 and 8), 30 (lanes 3 and 4, 9 and 10), or 60 min (lanes 5 and 6, 11 and 12) in the presence of excess cold methionine. Subsequently, cells were put on ice, and trypsin was added to either the apical side (Ap) or the basolateral side (Bl) of the cells. Cells were lysed and hemagglutinin was immunoprecipitated and analyzed by SDS gel electrophoresis. Arrowheads highlight the reduction in cleavage of hemagglutinin by trypsin added to the apical side, compared with that cleaved by trypsin added to the basolateral side in nocodazole-treated cells. (b) The percent surface expression of hemagglutinin on the apical domain (■) or the basolateral domain (▨), after 60 min of chase, was calculated as described in Methods. Shown are means ± SD. A decrease in apically expressed hemagglutinin in nocodazole-treated cells is responsible for the change in the apical-to-basolateral ratio of expressed hemagglutinin. A paired *t* test showed that the change in surface expression of hemagglutinin is significant in nocodazole-treated cells at the apical domain ($p < 0.001$, $n = 11$), but not significant at the basolateral domain ($p < 0.05$, $n = 11$).

supports with pores of 3.0 μm (see Methods). Cells were infected with VSV and treated with dimethyl sulfoxide (DMSO) or drugs. Arrival of newly synthesized VSV-G protein on the cell surface was detected with a cell-surface antibody-binding assay (Ploegh *et al.*, 1981; Pfeiffer *et al.*, 1985). By adding the anti-VSV-G antibody to either the apical or the basolateral side of the cells, the polarity of VSV-G expression could be assessed. After lysis and immunoprecipitation, the surface-exposed VSV-G was analyzed by SDS gel electrophoresis.

As shown in Figure 7a, pulse-labeled VSV-G was not precipitated by antibody added to the cell surface (lane 1), but, after a 60-min chase, VSV-G was detected by the extracellularly added antibody (Figure 7a, lanes 2 and 3). More VSV-G was detected when the antibody was added to the basolateral side of the cells (Figure 7a, lane 3), whereas only a small amount was detected by apically added antibody (Figure 7a, lane 2). In taxol- or nocodazole-treated cells, there was no appreciable change in the amount of VSV-G detected at either domain (Figure 7a, lanes 5 and 6, 8 and 9). The high apical fraction of VSV-G may represent the inherent background of the antibody assay; it does not reflect loss of cell polarity, because the polarity of hemagglutinin, as detected with the trypsin assay, is the same for cells grown on 3.0-μm pore supports as for cells grown on Millicell supports (data not shown). Quantitation showed that, within the detection limits of our assay, the amount of surface-expressed VSV-G was not affected by nocodazole or taxol (Figure 7b). The polarity of VSV-G delivery, as expressed by the basolateral to apical ratio, was also not changed by the drug treatment: all differences between control and drug-treated cells were nonsignificant as determined by a paired *t* test.

Thus, whereas polar expression of the apically targeted hemagglutinin was disrupted by microtubule-perturbing drugs, that of the basolaterally targeted VSV-G was unaffected.

Discussion

Microtubule perturbation inhibits transport to the apical cell surface

In this paper, we report the effects of microtubule-perturbing drugs on the transport of newly synthesized viral glycoproteins in MDCK cells. Perturbation of the microtubular cytoskeleton with either taxol or nocodazole inhibited delivery of hemagglutinin to the apical domain. The extent of inhibition by both drugs was similar. We

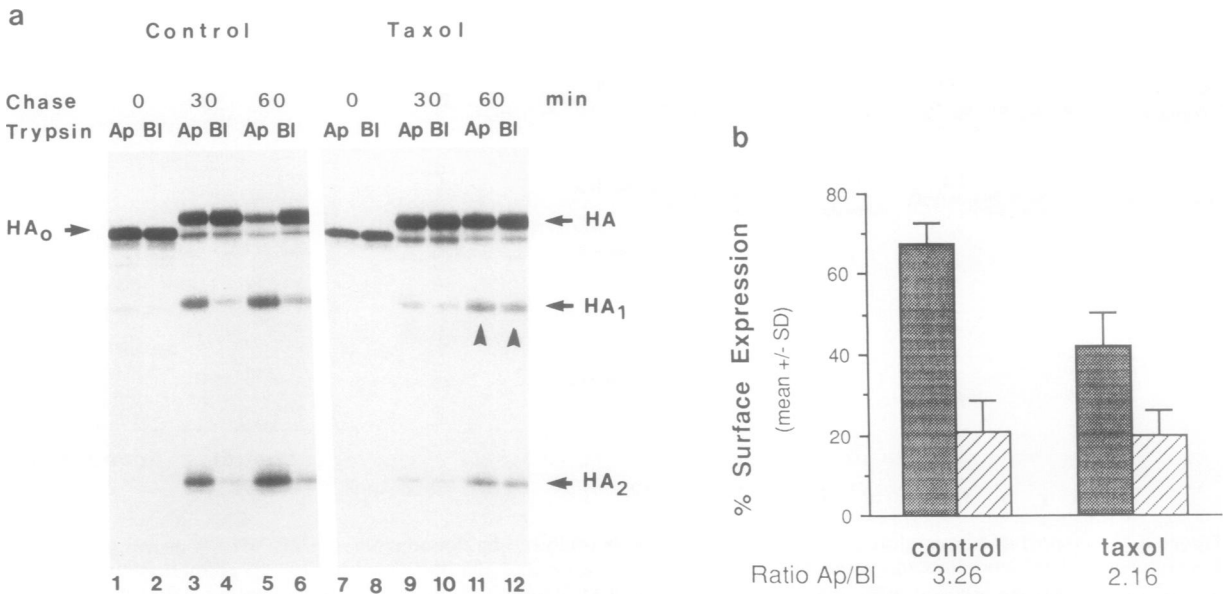

Figure 6. **Taxol inhibits transport of hemagglutinin to the apical domain.** (a) MDCK cells grown on Millicell HA culture supports were infected with influenza virus and treated with 0.1% DMSO (control) or 10 μM taxol for 4 h at 37°C before pulse labeling. After a 5-min pulse with 50 μCi [^{35}S]-methionine, cells were chased for 0 (lanes 1 and 2, 7 and 8), 30 (lanes 3 and 4, 9 and 10), or 60 min (lanes 5 and 6, 11 and 12). Subsequently, cells were put on ice, and trypsin was added to either the apical side (Ap) or the basolateral side (Bl) of the cells. Cells were lysed and hemagglutinin was immunoprecipitated and analyzed by SDS gel electrophoresis. Arrowheads highlight the reduction in cleavage of hemagglutinin by trypsin added to the apical side, compared with that cleaved by trypsin added to the basolateral side in taxol-treated cells. (b) The percent surface expression of hemagglutinin on each domain after 60 min of chase was calculated as described in Methods. Shown are means ± SD. A paired *t* test showed that taxol changed the surface expression of hemagglutinin significantly at the apical domain ($p < 0.001$, $n = 10$), but not significantly at the basolateral domain ($p < 0.01$, $n = 10$).

saw no evidence that the drug treatments led to missorting of hemagglutinin to the basolateral domain, as measured by a biochemical assay. Electron microscopic examination of infected and drug-treated MDCK cells also failed to demonstrate significant budding of influenza virions on the basolateral domain (unpublished observations). In contrast, our experiments did not reveal any interruption of delivery of VSV-G to the basolateral domain after administration of microtubule-perturbing drugs.

Our results are in general agreement with those of several laboratories, which state that microtubules play a role in the correct transport of apically targeted glycoproteins in polarized epithelial cells, but not of the basolaterally targeted ones (Rindler *et al.,* 1987; Achler *et al.,* 1989; Eilers *et al.,* 1989; Parczyk *et al.,* 1989). In particular, our observation that hemagglutinin accumulates intracellularly in drug-treated cells is quite comparable with that of Eilers *et al.* (1989), who found that nocodazole inhibited transport of aminopeptidase and lysosomal hydrolases to the apical surface in Caco-2 cells.

Our finding that detectable quantities of hemagglutinin are not missorted to the basolateral domain differs somewhat with the results of others. Parczyk *et al.* (1989) found that nocodazole and colchicine cause missorting of two secretory proteins from the apical to basolateral domain in MDCK cells. In addition, in the experiments of Eilers *et al.* (1989), a fraction of the aminopeptidase that was prevented by drug-treatment from reaching the apical surface was detected on the basolateral domain. Most significantly, Rindler *et al.* (1987) observed increased amounts of influenza hemagglutinin and budding virions on the basolateral domain of MDCK cells treated with nocodazole and taxol.

We do not consider these apparent discrepancies to be at odds with our own data. Instead, we think it likely that proteins induced to accumulate on the exocytic pathway may eventually reach the basolateral domain through default. Such missorting may be more likely with untethered secretory proteins than with membrane proteins, but it may also be possible with membrane proteins. In the case of Rindler *et al.* (1987), it is possible that differences in influenza strain and specific experimental conditions were sufficient to permit a fraction of the hemagglutinin to be transported to the basolateral side (see below).

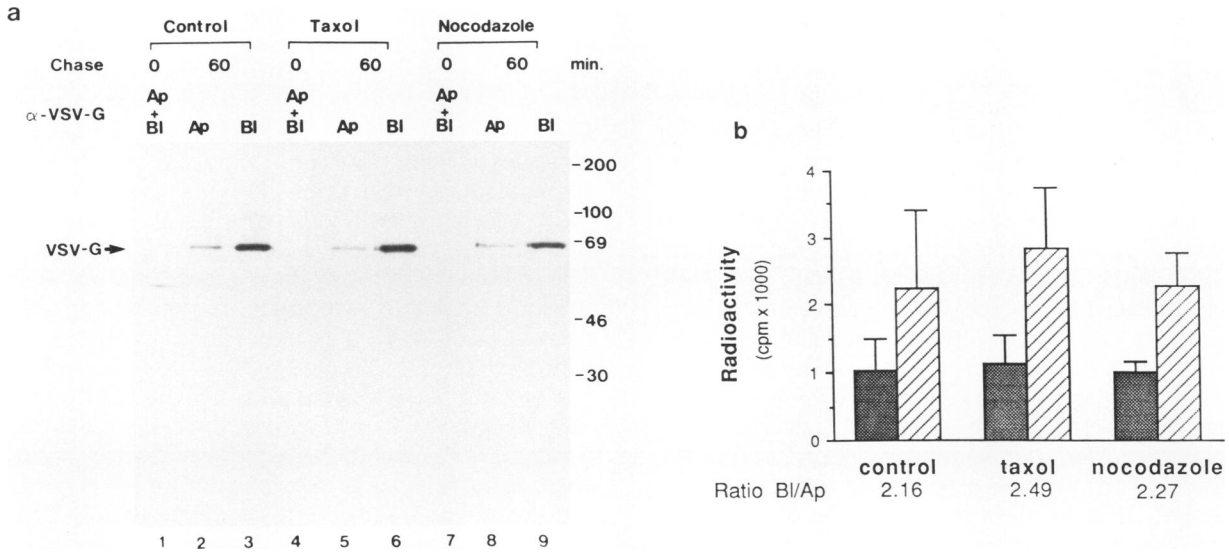

Figure 7. **The polarity of VSV-G expression is not altered after drug treatment.** (a) MDCK cells grown on Transwell culture supports were infected with VSV and treated with 0.1% DMSO for 4 h (lanes 1–3), 10 μM taxol for 4 h (lanes 4–6), or 10 μg/ml nocodazole for 1 h (lanes 7–9) at 37°C. Cells were labeled by a 10-min pulse with 50 μCi [^{35}S]-methionine and put on ice right away (0 min) or after a 60-min chase in the presence of excess unlabeled methionine (60 min). A VSV-G antiserum was applied either to the apical (Ap) or the basolateral (Bl) side of the cells, or both (Ap + Bl). After lysis, the VSV-G antibody complexes were precipitated and the samples analyzed by SDS gel electrophoresis. Neither taxol nor nocodazole altered the amount of VSV-G detected by antibody added to either side of the cells. (b) The radioactivity in each VSV-G band was quantitated as described in Methods. The means ± SD of six (control and taxol) or four (nocodazole) experiments are shown. A paired *t* test showed that neither taxol nor nocodazole affects the expression of VSV-G at the basolateral domain (▨; taxol: $p < 0.2$; nocodazole: $p < 0.1$). The difference in apically detectable VSV-G is nonsignificant (■; taxol: $p < 0.1$; nocodazole: $p < 0.1$). P values this high indicate a nonsignificant difference between controls and drug-treated cells and hence identical VSV-G expression.

On first examination, our results and those of others appear to be in direct contradiction with those of Salas *et al.* (1986), who reported no effects of colchicine, nocodazole, or taxol on epithelial polarity in viral-infected MDCK cells. However, these authors did report a reduction in the amount of influenza virus budding from the apical surface, as well as a decrease of the amount of hemagglutinin on the apical cell surface, with both colchicine and taxol (see Salas *et al.,* 1986, Tables I and IV). It seems likely, therefore, that in the experiments of Salas *et al.* (1986), as in our experiments, treatment with microtubule-active drugs resulted in an inhibition of hemagglutinin transport to the apical surface.

Subpopulations of microtubules involved in protein transport

The concentration of nocodazole at which microtubules began to depolymerize, as judged by immunofluorescence, did not correspond with the nocodazole concentration at which the inhibition of transport was observed. Whereas concentrations ≥ 0.1 μg/ml nocodazole depolymerized microtubules, a decrease in delivery of hemagglutinin to the apical cell surface was only observed at concentrations of 1 μg/ml or higher (data not shown). Conversely, after treatment with 10 μg/ml nocodazole, a concentration that inhibits apical hemagglutinin expression, some microtubules remained. Most of these nocodazole-resistant microtubules were found in the apical cap in MDCK cells, although some could also be found in other parts of the cells. When nocodazole treatment was combined with low-temperature incubation of the cells, nearly all microtubules were depolymerized; inhibition of hemagglutinin transport, however, was not increased (unpublished observation). Similar findings have been previously reported for gp80 (Parczyk *et al.,* 1989), an endogenous protein secreted primarily from the apical surface of MDCK cells. These results suggest that a certain subset of microtubules (those that depolymerize at concentrations between 1 and 10 μg/ml nocodazole) are required to ensure correct delivery of hemagglutinin to the apical membrane of MDCK cells. Subpopulations of microtubules that were characterized by differential posttranslational modifications of tubulin, such as detyrosination and acetylation, have been demonstrated (Bré *et al.,* 1987; Pi-

perno *et al.,* 1987; Bulinski *et al.,* 1988). Whether the nocodazole-sensitive subset of microtubules involved in apical transport in MDCK cells possesses these biochemical characteristics, such as detyrosination or acetylation, has not been investigated by us. In neuronal cells, evidence for separate roles for subsets of microtubules has been found (Miller *et al.,* 1987). In this study, a subpopulation of axonal microtubules was shown to carry all the vesicles, whereas other microtubules in the same axon were shown to have an architectural function.

The onset of hyperpolymerization of microtubules by taxol at 1 μM did coincide with the manifestation of inhibition of hemagglutinin transport (data not shown). Concentrations below 1 μM taxol failed to cause detectable hyperpolymerization of microtubules or inhibition of hemagglutinin transport. Subtle differences, however, may have escaped our detection.

The two applied drugs, nocodazole and taxol, although having opposite effects on the polymerization state of tubulin, both inhibited the surface expression of hemagglutinin to a similar extent. A possible explanation for this similarity could be that merely perturbing the equilibrium that exists in the cell between polymerization and depolymerization of microtubules interferes with the proper functioning of microtubules in protein transport.

Intracellular location of arrested viral glycoproteins in nocodazole- or taxol-treated cells

Oligosaccharide-processing enzymes have distinct locations in eukaryotic cells (Kornfeld and Kornfeld, 1985). Therefore, the extent of oligosaccharide processing of glycoproteins can be used as an indicator of their intracellular location. From the differences in glycosylation patterns between taxol- and nocodazole-treated cells, one might conclude that nocodazole inhibited the glycosylation machinery. This explanation can be ruled out because the VSV-G protein and other glycoproteins are unaffected in their glycosylation by microtubule-perturbing drugs (our unpublished observations; Rogalski *et al.,* 1984, Stults *et al.,* 1989). Instead, we believe that hemagglutinin accumulates in nocodazole-treated cells at an early stage of the transport pathway. This could be either the endoplasmic reticulum, the cis-Golgi, or anywhere in between (Kornfeld and Kornfeld, 1985). Because VSV-G traverses the pathway between the endoplasmic reticulum and the Golgi complex normally in nocodazole-treated cells, it is unlikely that vesicle movement itself along this part of the pathway is dependent on microtubules. Rather, it is probable that nocodazole-induced events taking place at the Golgi complex affect intracellular transport upstream in the biosynthetic pathway. Hemagglutinin failing to exit the Golgi complex could prevent new hemagglutinin from entering. This results in the incomplete processing of hemagglutinin. The effect of nocodazole on the glycosylation of hemagglutinin is most likely secondary, whereas the primary effect of nocodazole is on the Golgi complex and its role in apical vesicle transport. Whether this is hemagglutinin-specific or a general consequence for all apical glycoproteins is unknown. To our knowledge, this is the first time that an inhibition of protein transport to the cell surface caused by microtubule-perturbing drugs has been directly correlated with the stage of processing.

An explanation for this remarkable difference between nocodazole and taxol treatment could be sought in the remaining associations between the Golgi complex and the microtubule structures in drug-treated cells. Morphological data obtained by several authors (Wehland *et al.,* 1983; Rogalski and Singer, 1984; Thyberg and Moskalewski, 1985) who used Golgi-specific markers showed that Golgi stacks in nocodazole-treated cells are scattered throughout the cytoplasm. In taxol-treated cells the Golgi complex was disorganized, but not completely dispersed, and was associated with the microtubules in the cell periphery. Perhaps the remaining association of the Golgi complex with microtubules in taxol-treated cells was important in allowing the hemagglutinin to progress to the trans-Golgi.

Influence of the growth substratum on microtubular organization and protein transport in MDCK cells

We found that the choice of substratum had a dramatic effect on the ability of taxol to inhibit hemagglutinin transport. In cells grown on plastic substrata, taxol did not inhibit hemagglutinin transport, whereas in cells grown on permeable substrata the inhibition of hemagglutinin transport was similar in magnitude to nocodazole-induced inhibition.

These observations might be correlated with the architecture of the microtubular cytoskeleton in MDCK cells grown on these different types of substrata. In MDCK cells the microtubular cytoskeleton has been shown to reorganize dramatically during cell polarization. As reported by Bacallao *et al.* (1989), microtubules emanate mainly from a juxtanuclear centrosome

in subconfluent cells grown on permeable substrata. As the cells pack more closely together and the cell height increases, the arrangement of microtubules no longer depends on a single organizing center. Instead, the microtubules become highly polarized along the apical-to-basal axis. Lateral microtubules run vertically with their minus ends in the apical part of the cells, and at the base of the cells there is a loose network.

Cells grown on both types of growth substrata had an apical cap of microtubules. The lateral microtubules in cells grown on a permeable support were well organized along the apical-basal axis, whereas those in cells grown on glass ran more parallel to the substratum, somewhat reminiscent of the microtubules in 3-d-old MDCK cells grown on permeable supports (Bacallao *et al.,* 1989). This suggests that cells grown on solid supports do not progress fully into a very tall, cuboidal epithelium as they do on permeable supports. The reasons for this are unknown, but may have to do with the capacity of cells grown on permeable supports to take up nutrients from the basolateral side of the cells, better reflecting in vivo physiological conditions (Simons and Fuller, 1985). Also, the basal plasma membrane is flat on plastic surfaces (Salas *et al.,* 1986), whereas numerous basal protrusions can be observed when cells are cultured on nitrocellulose acetate filters (Matlin and Simons, 1984). These different cell-substrate interactions could give rise to signals that determine the final morphology of the cells.

Our results suggest that the microtubular cytoskeleton in cells grown on solid or permeable substrata differ from each other in architecture. Such differences could be part of the reason that, in one study with MDCK cells grown on collagen (Rindler *et al.,* 1987), increased budding of influenza virions at the basolateral domain was observed. The molecular nature of the interactions of MDCK cells with the growth substratum is unknown, and the intracellular effects of the growth substratum on the cytoskeleton cannot yet be evaluated.

Functional role of microtubules

What conclusions can we draw from these results with respect to the role of microtubules in protein sorting? Sorting of plasma membrane components in MDCK cells takes place after apically and basolaterally targeted proteins arrive in the Golgi complex (Matlin and Simons, 1984; Matlin, 1986a; Griffiths and Simons, 1986). It involves the recognition of the proteins to be sorted, segregation of the recognized proteins, and lastly, delivery of the segregated proteins to their final destinations (Caplan and Matlin, 1989).

Several observations indicate that the recognition and segregation steps in epithelial cells do not depend on an intact microtubular cytoskeleton. First, the apically targeted hemagglutinin is only retarded, and in our study almost all of it eventually reaches the correct apical domain. Second, the delivery of basolateral proteins is normal when the microtubular cytoskeleton is perturbed. And third, both the secretory proteins sorted to the apical domain, and the apical component of proteins normally secreted from both domains, are similarly inhibited by microtubule-depolymerizing drugs (Parczyk *et al.,* 1989). Furthermore, glycolipids are still correctly sorted in MDCK cells treated with nocodazole, although their transport is retarded (G. van Meer, personal communication). All these results point to a role for microtubules at the stage of delivery and not in the earlier steps of recognition and segregation (Caplan and Matlin, 1989).

The role of microtubules in delivery of proteins can be envisioned in several ways. In analogy to the directly visualized transport of organelles along microtubules in axonal transport, microtubules could serve as tracks (Schnapp *et al.,* 1985; Vale *et al.,* 1985). The well-oriented microtubules in MDCK cells, with their minus ends towards the apical side of the cell, seem ideal tracks for organelle transport (Bacallao *et al.,* 1989). This transport could be facilitated by molecular motors, like kinesin or cytoplasmic dynein, that have been shown to promote movement in opposite directions along microtubules in vitro (Vale *et al.,* 1985; Paschal and Vallee, 1987). Alternatively, a function for microtubules as targets for transport vesicles could be envisioned. Vesicles destined for the apical domain, diffusing from the Golgi area, could associate with the dense apical cap and be brought close enough to the apical membrane for fusion to occur. Even though interaction of vesicles containing transported proteins with microtubules has been implied (Van der Sluijs *et al.,* 1989), evidence for the movement of vesicles containing newly synthesized proteins along microtubules has yet to be provided. If these mechanisms exist, they are most likely only applicable to delivery of proteins to the apical plasma membrane in MDCK cells, because proteins do not appear to depend on microtubules for delivery to the basolateral domain.

In addition to these two mechanisms, a function for microtubules in protein transport could

also be as a structural framework for the architecture of the cytoplasm, with a central role for the Golgi complex. One of the most obvious morphological changes that takes place after treatment of cells with a microtubule-depolymerizing drug such as nocodazole is the dissociation of the Golgi complex. The intricate interaction between Golgi components and microtubules becomes even more evident when nocodazole is washed away and the reorganization of the Golgi complex is observed. Under those conditions, the repolymerization of microtubules can be seen to precede the reorganization of the Golgi complex (Ho *et al.*, 1989; Turner and Tartakoff, 1989). Also, the differentiation of the microtubular cytoskeleton after MDCK cells reach confluence is accompanied by a relocalization of the Golgi complex to the apical part of the cell (Bacallao *et al.*, 1989). These data, combined with the inhibition of apical protein transport after microtubule perturbation, indicate that the association of microtubules with the Golgi complex is intricately connected to its function in apical protein transport. The role of microtubules in protein transport could be to position the Golgi complex in the apical part of the cell or, at a molecular level, to aid the exit of the apical proteins from the Golgi complex. More information about the connections of the microtubules with the Golgi membranes is needed to answer these questions.

The orientation of the lateral microtubules with their minus ends in the apical part of MDCK cells points to the presence of some microtubule-organizing activity in the apical cytoplasm (Bacallao *et al.*, 1989). In turn, the polar organization of the Golgi complex is critical to the ability of the cell to correctly transport proteins to the apical domain of the cell. Knowledge of how the polarity of the cytoplasm is established and maintained is key to understanding the mechanisms involved in polarized protein transport.

Methods

Materials

DMSO was purchased from Baker (Phillipsburg, NJ) and nocodazole from Aldrich Chemical (Milwaukee, WI). Taxol was donated by Dr. M. Suffness, National Product Branch, Division of Cancer Treatment, National Cancer Institute. MDCK cells were grown on plastics from Falcon or on permeable substrata (Millicell HA inserts, Millipore, Bedford, MA; or Transwells, Costar, Cambridge, MA). Culture media were from Gibco Laboratories, Grand Island, NY.

Cells

MDCK cells exhibiting low trans-monolayer resistance (MDCK II) were used. Maintenance of stock cells and experimental conditions for growth on plastic were as described (Matlin and Simons, 1983).

For most experiments examining the polarity of hemagglutinin expression, MDCK cells were grown on 12-mm Millicell HA permeable supports with 0.45-μm pores. Cells were seeded at 1.3×10^5 cells/cm^2, fed every other day, and used on the fourth day.

To permit infection with VSV from the basal surface, MDCK cells were cultured in Transwells with 3.0-μm pores (Fuller *et al.*, 1984). Because the cells did not proliferate well on this substratum, it was necessary to seed cells at high density (1.2×10^6 cells/cm^2 on 6.5-mm-diam Transwells) and to culture them for 5 d to achieve a confluent monolayer. MDCK cells grown on large-pore Transwells have a polarized phenotype similar to cells grown on Millicell HA permeable supports, as judged by the morphology of the microtubular cytoskeleton and the polarity of hemagglutinin expression.

Baby hamster kidney (BHK) cells were grown in Glasgow minimum essential medium (MEM), 10% (w/v) tryptose-phosphate, 5% (v/v) fetal bovine serum as described (Burke *et al.*, 1982).

Viruses

Influenza virus strain A/PR/8/34 (H1 subtype; PR8), plaque-purified on MDCK cells, was used. Stocks were grown in embryonated chicken eggs as described (Skibbens *et al.*, 1989).

For experiments with VSV (Indiana serotype; White *et al.*, 1981), viral stocks were grown in BHK cells as described by Matlin *et al.* (Matlin *et al.*, 1982) for MDCK cells.

Both influenza virus and VSV were titrated on MDCK cells (Matlin *et al.*, 1981, 1982).

Antibodies

Appearance of VSV-G protein on the cell surface was detected with a polyclonal rabbit serum raised against a Triton X-114 extract of purified virions. Influenza hemagglutinin was immunoprecipitated with culture supernatants of the mouse monoclonal H28E23 (Skibbens *et al.*, 1989). A culture supernate of the mouse monoclonal B-5-1-2, directed against α-tubulin (Piperno *et al.*, 1987), was used for immunofluorescence of the microtubular cytoskeleton and detection of tubulin by Western blotting. Secondary antibodies for immunofluorescence and western blots (FITC- or horseradish peroxidase (HRP)-conjugated, respectively) were from TAGO, Burlingame, CA.

Drug treatments

Stock solutions of taxol and nocodazole were stored at −20°C in DMSO at 10 mM and 10 mg/ml, respectively. Unless otherwise stated, the drugs were diluted 1:1000 into the appropriate buffers or media, supplemented with 0.2% (w/v) bovine serum albumin (BSA; final concentrations: 10 μg/ml nocodazole, 10 μM taxol). BSA was added to all media to prevent precipitation of nocodazole (G. van Meer, personal communication). Controls received 0.1% (v/v) DMSO, unless otherwise stated.

In most experiments, cells were pretreated with Earle's minimal essential medium (EMEM) containing 0.2% (w/v) BSA, 10 mM HEPES (*N*-2-hydroxyethylpiperazine-*N*′-2-ethanesulfonic acid), pH 7.3, penicillin-streptomycin (EMEM; infection medium) containing nocodazole for 1 h or taxol for 4 h before pulse-labeling, fixation for immunofluorescence, or extraction for tubulin analysis. Controls were treated for equivalent times with DMSO alone. In labeling experiments, drugs were present continuously throughout the pulse and chase incubations. Drugs were also included in the Triton X-100 containing extraction buffer used to analyze the po-

lymerization state of tubulin. The total time of drug exposure varied depending on the particular experiment.

Immunofluorescence

To examine the morphology of the microtubular cytoskeleton by immunofluorescence, we grew MDCK cells either on glass coverslips under conditions described for growth on plastic or on Millicells. For observation by confocal laser microscopy, we treated MDCK cells with drugs or DMSO in EMEM, washed them with PME buffer (80 mM piperazine-*N,N'*-bis(2-ethanesulfonic acid) [PIPES], pH 6.8, 5 mM ethylene glycol-bis(β-aminoethyl ether)-*N,N,N',N'*-tetraacetic acid [EGTA], and 1 mM $MgCl_2$) (Bré *et al.,* 1987) containing drugs or DMSO at 37°C, and permeabilized them for 10 s (for glass coverslips) or 5 min (for Millicells) in PME containing 0.5% (w/v) Triton X-100 at 37°C. After rinsing once in PME, cells were fixed using the pH shift paraformaldehyde fixation as described (Bacallao and Stelzer, 1989; Berod *et al.,* 1981). In short, cells were fixed with 3% (w/v) paraformaldehyde, first in PME at pH 6.8, then at pH 11.0 in 100 mM sodium borate. After quenching with 1 mg/ml sodium borohydride in phosphate-buffered saline (PBS) without cations, pH 8.0, coverslips were incubated with the anti-α-tubulin and fluorescein isothiocyanate (FITC)-secondary antibodies as described (Skibbens *et al.,* 1989). The Millicell HA culture supports were prepared for immunofluorescence as described (Bacallao *et al.,* 1989; Bacallao and Stelzer, 1989), using the antibodies mentioned above. Specimens were viewed with the MRC-500 confocal imaging system from Bio-Rad (Watford, UK), mounted on an Axiophot microscope (Zeiss, Oberkochen, FRG). Optical sections were taken along the *z*-axis at 2-μm increments. For reproduction, the images were optically enhanced using the scaling feature. By scaling all images from the same series by the same factor, the relative fluorescence between dim and bright sections was preserved. Pictures were photographed directly off a black-and-white monitor with Kodak Tmax 100 film. The exposure times and printing conditions for all images of the same series were identical.

Tubulin extraction and Western blots

To analyze biochemically the effects of nocodazole and taxol on tubulin polymerization, we washed cells treated with drugs or DMSO in EMEM, as described above, at 37°C with microtubule-stabilizing buffer (PMEG) (0.1 M PIPES, pH 6.75, 1 mM $MgSO_4$, 1 mM EGTA, and 2 M glycerol containing drugs or DMSO, and extracted them for 15 min at 37°C with PMEG containing 0.1% (w/v) Triton X-100. The supernatants, containing unpolymerized tubulin, were collected; the extraction was repeated; and supernatants from both extractions were pooled. Drugs and DMSO were present in all the buffers up to this point. The Triton X-100 insoluble residues containing polymeric tubulin were solubilized at room temperature for 5 min in 25 mM tris(hydroxymethyl)aminomethane (Tris), pH 7.4, 0.4 M NaCl, and 0.5% (w/v) sodium dodecyl sulfate (SDS) and passed through a 22-gauge needle several times to shear the DNA.

For gel electrophoresis and blotting, equal volumes of all samples (soluble and polymeric) were mixed with 1/5 volume of 5× concentrated sample buffer, boiled, and reduced. After alkylation, samples were run on 10% polyacrylamide gels as described above. The amount of protein in each sample was determined by a sensitive Coomassie dye binding assay (Bramhall *et al.,* 1969). Proteins were transferred from the gel to Immobilon membrane (Millipore) for 1 h at 15 V with the Genie apparatus (Idea Scientific, Corvallis, OR). The blots were processed as described by Burke *et al.* (1982), using 1:25 diluted anti-α-tubulin antibody B-5-1-2 as primary antibody and 1:200 diluted goat-anti-mouse-IgG, horseradish peroxidase conjugated (TAGO) as secondary antibody. Blots were developed with 0.5 mg/ml diaminobenzidine and 0.01% (v/v) H_2O_2 in 50 mM Tris, pH 7.4 (Burke *et al.,* 1982).

Pulse-chase experiments and cell–surface assay

Influenza virus. MDCK cells grown either on plastic dishes or on permeable substrata were infected with influenza virus, pulse-labeled with 50 μCi [^{35}S]-methionine, and chased in medium containing excess unlabeled methionine as described previously (Matlin and Simons, 1983, 1984; Matlin, 1986b). In most cases, nocodazole-treated cells were infected for 3.5 h and taxol-treated cells for 6.5 h before pulse-labeling. Arrival of hemagglutinin on the cell surface was monitored by treatment with extracellular trypsin at 0°C as described (Matlin *et al.,* 1983; Matlin, 1986b). The ability of trypsin to reach the basolateral plasma membrane through the filter was demonstrated by increasing the trypsin concentration, which failed to increase the amount of hemagglutinin cleaved. Also, increasing the pore size to 3.0 μm (Transwell supports), did not lead to an increase in cleaved hemagglutinin after trypsin addition to the basolateral side of control or drug-treated cells (data not shown).

After pulse-labeling and trypsinization, cells were extracted at 4°C with 1 ml of 20 mM Tris, pH 8.6; 150 mM NaCl; 1% (w/v) Triton X-100; 0.1% (w/v) SDS; and a protease inhibitor cocktail consisting of 1 mM phenylmethylsulfonylfluoride (PMSF), 10 μg/ml aprotonin, 17 μg/ml benzamidine, 1 μg/ml pepstatin, and 0.1 μg/ml antipain. The insoluble residue was removed by centrifugation for 5 min at full speed in a microfuge. The Triton-SDS mixture solubilized all hemagglutinin, including the fraction that is not extracted by solutions of Triton X-100 alone (Skibbens *et al.,* 1989). The extraction solution was added either directly to the plastic culture dish or, in the case of Millicells and Transwells, the permeable supports were excised with a cork bore and extracted in a 1.5-ml microfuge tube.

Hemagglutinin was immunoprecipitated by addition of saturating amounts of anti-hemagglutinin antibody. After an overnight incubation at 4°C, the immune complexes were precipitated by addition of 25 μl Protein A-Trisacryl (50% slurry, Pierce Chemical, Rockford, IL) for 2 h at 4°C. The immunoprecipitates were washed four times in 10 mM Tris, pH 8.6, 0.5 M NaCl, 1% (w/v) Triton X-100, 0.1% (w/v) SDS.

To analyze the immunoprecipitates by SDS gel electrophoresis, hemagglutinin was released from the Trisacryl beads by heating to 95°C for 3 min in 15-μl gel sample buffer (50 mM Tris, pH 8.8, 5 mM EDTA, 4% [w/v] SDS, 10% [w/v] sucrose, 10 mM dithiotreitol), alkylated by incubation with 100 mM iodoacetamide at 37°C for 15 min, and separated on SDS polyacrylamide gels. Gels were prepared and run as described previously (Piccioni *et al.,* 1982), using the Laemmli system (Laemmli, 1970), and fluorographed with Enhance (New England Nuclear, Boston, MA).

VSV. To monitor the transport and sorting of VSV-G, MDCK cells on 3.0-μm-pore Transwell supports were infected with VSV at 40 pfu/cell in 200 μl EMEM added to the basolateral side of the cells; 100 μl EMEM was present on the apical side. After 1 h, the medium was aspirated from both sides of the cells and replaced with 200 μl EMEM on the apical side and 700 μl on the basolateral side. DMSO and taxol were introduced at this stage and nocodazole 3 h later, so that the drugs were present for 4 and 1 h, respectively. After 5 h of total infection, the cells were pulse-labeled and chased as described for the Millicell HA supports (Matlin, 1986b).

Appearance of VSV-G on the cell surface was detected by antibody precipitation essentially as described by Pfeiffer *et al.* (1985; see also Ploegh *et al.,* 1981). In brief, infected

and labeled cells grown on Transwells were placed on 25-μl drops of PBS containing calcium and magnesium (Dulbecco's formula; PBS$^+$) and 10% (v/v) newborn calf serum (Sigma, St Louis, MO) (PBS$^+$/NCS) on a sheet of Parafilm in an inverted lid of a 24-well plate; 25 μl PBS$^+$/NCS was added to the apical side. On the appropriate side(s) of the cells, 2 μl of anti-VSV-G serum was included in the PBS$^+$/NCS. After 1 h on ice, the culture supports were returned to the wells and washed extensively (10 times) with cold PBS$^+$/NCS to remove unbound antibody (700 μl basolateral, 200 μl apical). The culture supports were then punched out with a cork bore and extracted for 15 min on ice in a 1.5-μl vial, containing 500 μl of 20 mM Tris, pH 7.4, 150 mM NaCl, 1% (w/v) Triton X-100, and the same protease inhibitor cocktail as described above. The filters and the insoluble residues were spun down in a microfuge at full speed for 5 min. The supernatants were mixed with 25 μl Protein A-Trisacryl and inverted for 1 h at 4°C. Immunoprecipitates were washed and analyzed by SDS gel electrophoresis as described above for hemagglutinin.

Quantitation and statistical analysis

To quantitate the amount of surface expression, we cut hemagglutinin and VSV-G bands from dried gels, using the autoradiograph as a template, and counted them as previously described (Matlin and Simons, 1983).

For hemagglutinin it was possible to calculate the percent surface expression by comparing the amount of radioactivity in cleaved hemagglutinin with the total hemagglutinin radioactivity in that lane. Hemagglutinin is synthesized in the endoplasmic reticulum as a 68 000-Da protein, HAo (nomenclature as in Matlin and Simons, 1983). During transport to the cell surface, hemagglutinin is modified in the Golgi complex, resulting in a band of higher apparent molecular weight (HA). Trypsin cleaves HA into two disulfide-linked subunits, HA1 and HA2, which can be resolved on an SDS gel. Because some HA2 is lost during immunoprecipitation (Skibbens *et al.,* 1989), it was necessary to calculate the total amount of radioactivity in cleaved hemagglutinin by tripling the amount of radioactivity in HA1; in the PR8 hemagglutinin serotype there are twice as many methionine residues in HA2 as in HA1. The percentage of cleaved hemagglutinin, calculated from a lane in which the sample was only pulse-labeled and not chased, was subtracted from all samples as a background value.

In the course of the studies described here, it was observed that the hemagglutinin produced by the plaque-purified isolate of influenza strain PR8 is partially cleaved in the absence of trypsin in cells grown on permeable substrata. In MDCK cells grown on plastic substrata, this cleavage in the absence of trypsin is not observed. This endogenous cleavage is probably accomplished by a protease located in the trans-Golgi (Matlin and Simons, 1983). One cannot discriminate between hemagglutinin cleaved by the endogenous protease and hemagglutinin cleaved by trypsin. However, we assume that the cell sorts endogenously cleaved and uncleaved hemagglutinin identically. This assumption is supported by the observation that localization of hemagglutinin by immunofluorescence in frozen sections of infected, filter-grown MDCK cells does not reveal any substantial basolateral fraction.

Because control samples without added trypsin were not included in all experiments, the values for both apical and basolateral cleavage, and thus the polarity ratios reported here, include the endogenous cleavage as an unsubtracted background (see Figures 5 and 6). Calculation of this background from other experiments suggests that it is about 24 ± 4.9% (n = 8). Subtraction of this background from the results shown in Figures 5 and 6 would produce an apical-to-basolateral ratio of >10:1. Inclusion of the endogenous cleavage in our calculations would, however, not alter our conclusions about the effects of microtubule-active drugs on hemagglutinin transport.

The percentage of hemagglutinin surface expression was derived from single-gel lanes. Therefore, individual samples are internally controlled and can be directly compared. Because VSV-G surface expression data consisted of immunoprecipitated raw counts, the statistical variation of the VSV-G data was greater than that of the internally controlled hemagglutinin data.

The difference in cell-surface expression between drug-treated and control cells was statistically evaluated using a paired *t* test (Eilers *et al.,* 1989).

Acknowledgments

We thank Gerrit van Meer (Department of Cell Biology, Medical School, University of Utrecht, The Netherlands) and Robert Bacallao (Division of Nephrology, University of California at Los Angeles Medical Center, Los Angeles, California) for the communication of unpublished results, Donna Kendall for technical assistance, and Gianni Piperno and Brian Burke for their generous gifts of antibodies. We appreciate the technical advice of Peter Hollenbeck, Lawrence Goldstein, and Lynn Jesaitis and thank Cora-Ann Schoenenberger and Fred Flitsch for critically reading the manuscript. The confocal microscope was purchased with a grant from the National Institutes of Health, Division of Research Resources.

Received: June 11, 1990.
Revised and accepted: September 3, 1990.

References

Achler, C., Filmer, D., Merte, C., and Drenckhahn, D. (1989). Role of microtubules in polarized delivery of apical membrane proteins to the brush border of the intestinal epithelium. J. Cell Biol. *109,* 179–189.

Bacallao, R., Antony, C., Dotti, C., Karsenti, E., Stelzer, E.H.K., and Simons, K. (1989). The subcellular organization of Madin-Darby canine kidney cells during the formation of a polarized epithelium. J. Cell Biol. *109,* 2817–2832.

Bacallao, R., and Stelzer, E.H.K. (1989). Preservation of biological specimens for observation in a confocal fluorescence microscope and operational principles of confocal fluorescence microscopy. Methods Cell Biol. *31,* 437–457.

Balch, W.E., Elliot, M.M., and Keller, D.S. (1986). ATP-coupled transport of vesicular stomatitis virus G protein between the endoplasmic reticulum and the Golgi. J. Biol. Chem. *261,* 14681–14689.

Berod, A., Hartman, B.K., and Pujol, J.F. (1981). Importance of fixation in immunohistochemistry: use of formaldehyde solutions at variable pH for the localization of tyrosine hydroxylase. J. Histochem. Cytochem. *29,* 844–850.

Bramhall, S., Noack, N., Wu, M., and Lowenberg, J.R. (1969). A simple colorimetric method for the determination of protein. Anal. Biochem. *31,* 146–148.

Bré, M-H., Kreis, T.E., and Karsenti, E. (1987). Control of microtubule nucleation and stability in Madin-Darby canine kidney cells: the occurrence of noncentrosomal, stable detyrosinated microtubules. J. Cell Biol. *105,* 1283–1296.

Bulinski, J.C., Richards, J.E., and Piperno, G. (1988). Post-translational modifications of α tubulin: detyrosination and acetylation differentiate populations of interphase microtubules in interphase cells. J. Cell Biol. *106,* 1213–1220.

Burke, B., Griffiths, G., Reggio, H., Louvard, D., and Warren, G. (1982). A monoclonal antibody against a 135-K Golgi membrane protein. EMBO J. *1,* 1621–1628.

Busson-Mabillot, S., Chambaut-Guerin, A.-M., Ovtracht, L., Muller, P., and Rossignol, B. (1982). Microtubules and protein secretion in rat lacrimal glands: localization of short-term effects of colchicine on the secretory process. J. Cell Biol. *95,* 105–117.

Caplan, M.J., and Matlin, K.S. (1989). Sorting of membrane and secretory proteins in polarized epithelial cells. In: Functional Epithelial Cells in Culture, ed. K.S. Matlin, and J. Valentich, New York: Alan R. Liss, 71–127.

De Brabander, M.J., Van der Veire, R.M.L., Aerts, F.E.M., Borgers, M., and Janssen, P.A.J. (1976). The effects of methyl[5-(2-thienylcarbonyl)-1H-benzimidazol-2-yl]carbamate, (R 17934; NSC 238159), a new synthetic antitumoral drug interfering with microtubules on mammalian cells cultured in vitro. Cancer Res. *36,* 905–916.

De Brabander, M., Geuens, G., Nuydens, R., Willebrords, R., and De Mey, J. (1981). Taxol induces the assembly of free microtubules in living cells and blocks the organizing capacity of the centrosomes and kinetochores. Proc. Natl. Acad. Sci. USA *78,* 5608–5612.

Eilers, U., Klumperman, J., and Hauri, H-P. (1989). Nocodazole, a microtubule-active drug, interferes with apical protein delivery in cultured intestinal epithelial cells (Caco-2). J. Cell Biol. *108,* 13–22.

Fuller, S., von Bonsdorf, C.-H., and Simons, K. (1984). Vesicular stomatitis virus infects and matures only through the basolateral surface of the polarized epithelial cell line, MDCK. Cell *38,* 65–77.

Griffiths, G., and Simons, K. (1986). The trans-Golgi network: sorting at the exit site of the Golgi complex. Science *234,* 438–443.

Ho, W.C., Allan, V.J., van Meer, G., Berger, E.G., and Kreis, T.E. (1989). Reclustering of scattered Golgi elements occurs along microtubules. Eur. J. Cell Biol. *48,* 250–263.

Horwitz, S.B., Lothstein, L., Manfredi, J.J., Mellado, W., Parness, J., Roy, S.N., Schiff, P.B., Sorbara, L., and Zeheb, R. (1986). Taxol: mechanism of action and resistance. Ann. NY Acad. Sci. *466,* 733–744.

Kornfeld, R., and Kornfeld, S. (1985). Assembly of asparagine-linked oligosaccharides. Annu. Rev. Biochem. *54,* 631–664.

Kreis, T.E. (1990). Role of microtubules in the organisation of the Golgi apparatus. Cell Motil. Cytoskeleton *15,* 67–70.

Laemmli, U.K. (1970). Cleavage of structural proteins during the assembly of the head of bacteriophage T4. Nature *227,* 683–685.

Lisanti, M.P., Le Bivic, A., Sargiacomo, M., and Rodriguez-Boulan, E. (1989). Steady state distribution and biogenesis of endogenous Madin-Darby canine kidney glycoproteins: evidence for intracellular sorting and polarized cell surface delivery. J. Cell Biol. *109,* 2117–2128.

Matlin, K.S., Reggio, H., Helenius, A., and Simons, K. (1981). Infectious entry pathway of influenza virus in a canine kidney cell line. J. Cell Biol. *91,* 601–613.

Matlin, K.S., Reggio, H., Helenius, A., and Simons, K. (1982). Pathway of vesicular stomatitis virus entry leading to infection. J. Mol. Biol. *156,* 609–631.

Matlin, K.S., Bainton, D.F., Pesonen, M., Louvard, D., Genty, N., and Simons, K. (1983). Transepithelial transport of a viral membrane glycoprotein implanted into the apical plasma membrane of Madin-Darby canine kidney cells. I. Morphological evidence. J. Cell Biol. *97,* 627–637.

Matlin, K.S., and Simons, K. (1983). Reduced temperature prevents transfer of a membrane glycoprotein to the cell surface but does not prevent terminal glycosylation. Cell *34,* 233–243.

Matlin, K.S., and Simons, K. (1984). Sorting of an apical plasma membrane glycoprotein occurs before it reaches the cell surface in cultured epithelial cells. J. Cell Biol. *99,* 2131–2139.

Matlin, K.S. (1986a). The sorting of proteins to the plasma membrane in epithelial cells. J. Cell Biol. *103,* 2565–2568.

Matlin, K.S. (1986b). Ammonium chloride slows transport of the influenza virus hemagglutinin but does not cause misorting in a polarized epithelial cell line. J. Biol. Chem. *261,* 15172–15178.

Miller, R.H., Lasek, R.J., and Katz, M.J. (1987). Preferred microtubules for vesicle transport in lobster axons. Science *235,* 220–222.

Parczyk, K., Haase, W., and Kondor-Koch, C. (1989). Microtubules are involved in the secretion of proteins at the apical cell surface of the polarized epithelial cell, Madin-Darby canine kidney. J. Biol. Chem. *264,* 16837–16846.

Paschal, B.M., and Vallee, R.B. (1987). Retrograde transport by the microtubule-associated protein MAP 1C. Nature *330,* 181–183.

Pfeiffer, S., Fuller, S.D., and Simons, K. (1985). Intracellular sorting and basolateral appearance of the G-protein of vesicular stomatitis virus in Madin-Darby canine kidney cells. J. Cell Biol. *101,* 470–476.

Piccioni, R., Bellemare, G., and Chua, N.-H. (1982). Methods of polyacrylamide gel electrophoresis in the analysis and preparation of plant polypeptides. In: Methods in Chloroplast Molecular Biology, ed. M. Edelman, R.B. Hallich, and N.-H. Chua, Amsterdam: Elsevier/North Holland, 985–1014.

Piperno, G., LeDizet, M., and Chang, X. (1987). Microtubules containing acetylated alpha-tubulin in mammalian cells in culture. J. Cell Biol. *104,* 289–302.

Ploegh, H.L., Orr, H.T., and Strominger, J.L. (1981). Biosynthesis and cell surface localization of nonglycosylated human histocompatibility antigens. J. Immunol. *126,* 270–275.

Rindler, M.J., Ivanov, I.E., and Sabatini, D.D. (1987). Microtubule-acting drugs lead to the nonpolarized delivery of the influenza hemagglutinin to the cell surface of polarized Madin-Darby canine kidney cells. J. Cell Biol. *104,* 231–241.

Rodriguez-Boulan, E., and Sabatini, D.D. (1978). Asymmetric budding of viruses in epithelial monolayers: a model system for study of epithelial polarity. Proc. Natl. Acad. Sci. USA *75,* 5071–5078.

Rodriguez-Boulan, E., and Pendergast, M. (1980). Polarized distribution of viral envelope glycoproteins in the plasma membrane of infected epithelial cells. Cell *20,* 45–54.

Rodriguez-Boulan, E., and Nelson, W.J. (1989). Morphogenesis of the polarized epithelial cell phenotype. Science *245,* 718–725.

Rogalski, A.A., Bergmann, J.E., and Singer, S.J. (1984). Effect of microtubule assembly status on the intracellular processing and surface expression of an integral protein of the plasma membrane. J. Cell Biol. *99,* 1101–1109.

Rogalski, A.A., and Singer, S.J. (1984). Associations of elements of the Golgi apparatus with microtubules. J. Cell Biol. *99,* 1092–1100.

Salas, P.J.I., Misek, D.E., Vega-Salas, D.E., Gundersen, D., Cereijido, M., and Rodriguez-Boulan, E. (1986). Microtubules and actin filaments are not critically involved in the biogenesis of epithelial cell surface polarity. J. Cell Biol. *102,* 1853–1867.

Schnapp, B.J., Vale, R.D., Sheetz, M.P., and Reese, T.S. (1985). Single microtubules from squid axoplasm support bidirectional movement of organelles. Cell *40,* 455–462.

Simons, K., and Fuller, S.D. (1985). Cell surface polarity in epithelial cells. Annu. Rev. Cell Biol. *1,* 243–288.

Skibbens, J.E., Roth, M.G., and Matlin, K.S. (1989). Differential extractibility of influenza hemagglutinin during intracellular transport in polarized epithelial cells and non-polar fibroblasts. J. Cell Biol. *108,* 821–832.

Stults, N.L., Fechheimer, M., and Cummings, R.D. (1989). Relationship between Golgi architecture and glycoprotein biosynthesis transport in chinese hamster ovary cells. J. Biol. Chem. *264,* 19956–19966.

Thyberg, J., and Moskalewski, S. (1985). Microtubules and the organization of the Golgi complex. Exp. Cell Res. *159,* 1–16.

Turner, J.R., and Tartakoff, A.M. (1989). The response of the Golgi complex to microtubule alterations: the roles of metabolic energy and membrane traffic in Golgi complex organization. J. Cell Biol. *109,* 2081–2088.

Vale, R.D., Schnapp, B.J., Mitchison, T., Steuer, E., Reese, T.S., and Sheetz, M.P. (1985). Different axoplasmic proteins generate movement in opposite directions along microtubules in vitro. Cell *43,* 623–632.

Van der Sluijs, P., Bennett, M.K., Antony, C., Simons, K., and Kreis, T.E. (1989). Binding of trans-Golgi network-derived exocytic carrier vesicles to microtubules in vitro. J. Cell Biol. *109,* 82a.

Wehland, J., Henkart, M., Klausner, R., and Sandoval, I.V. (1983). Role of microtubules in the distribution of the Golgi apparatus: effect of taxol and microinjected anti-α-tubulin antibodies. Proc. Natl. Acad. Sci. USA *80,* 4286–4290.

White, J., Matlin, K.S., and Helenius, A. (1981). Cell fusion by semliki forest, influenza, and vesicular stomatitis viruses. J. Cell Biol. *89,* 674–679.